nature structural & molecular biology

Purified Argonaute2 and an siRNA form recombinant human RISC

Fabiola V Rivas[1,3], Niraj H Tolia[1–3], Ji-Joon Song[1–3], Juan P Aragon[1], Jidong Liu[1], Gregory J Hannon[1] & Leemor Joshua-Tor[1,2]

Genetic, biochemical and structural studies have implicated Argonaute proteins as the catalytic core of the RNAi effector complex, RISC. Here we show that recombinant, human Argonaute2 can combine with a small interfering RNA (siRNA) to form minimal RISC that accurately cleaves substrate RNAs. Recombinant RISC shows many of the properties of RISC purified from human or *Drosophila melanogaster* cells but also has surprising features. It shows no stimulation by ATP, suggesting that factors promoting product release are missing from the recombinant enzyme. The active site is made up of a unique Asp-Asp-His (DDH) motif. In the RISC reconstitution system, the siRNA 5′ phosphate is important for the stability and the fidelity of the complex but is not essential for the creation of an active enzyme. These studies demonstrate that Argonaute proteins catalyze mRNA cleavage within RISC and provide a source of recombinant enzyme for detailed biochemical studies of the RNAi effector complex.

RNA interference or RNAi denotes a group of sequence-specific gene silencing pathways that can inhibit gene expression through a variety of different effector mechanisms[1]. RNAi is initiated upon the production of small, ~22-nucleotide (nt) double-stranded RNAs through the action of ribonuclease III family proteins. These small RNAs enter the RNAi effector complex, RISC, and serve as a guide to selection of silencing targets based on sequence complementarity[1]. RISC can silence its targets by RNA cleavage, by preventing protein synthesis or by triggering chromatin remodeling and consequent transcriptional repression. Of these repression modes, only siRNA-directed mRNA cleavage has been reproduced in cell free extracts and used as an assay for purifying RISC. Such efforts have led to the identification of complexes ranging from 160 kDa to 80S, depending on the extract source and the purification procedure[2–5]. Several proteins have been suggested to function as components of these complexes; however, two core elements have been found in all RISC purifications thus far. These are the small RNA guide and an Argonaute family protein. Recent biochemical, genetic and structural studies have suggested a model in which the core activities of RISC could be contributed by these two factors[6–8].

The crystal structure of an Argonaute protein from *Pyrococcus furiosus*[8] (PfAgo) revealed that one of the two signature domains of Argonaute family proteins, the PIWI domain, is similar to RNase H, with conserved active site aspartates, strongly implicating Argonaute as the element contributing siRNA-directed mRNA cleavage or 'slicer' activity. The enzyme is composed of a crescent-shaped base made up of the N-terminal, middle and PIWI domains. The PAZ domain, the second Argonaute signature domain, is held above the base by a 'stalk'-like region. Furthermore, the *P. furiosus* protein contains conserved aspartates, which in related nucleases and transposases are important for catalytic activity. The crystal structure of a Piwi-domain protein from another archaebacterium, *Archaeoglobus fulgidus*, was also recently determined[9]. This protein is composed of a Piwi and a mid domain that are structurally very similar to those in PfAgo with a slight difference in their relative orientation.

Several known characteristics of mRNA cleavage by RISC are consistent with an RNase H–like enzyme, namely the formation of a 5′ product with a 3′ hydroxyl and a 3′ product with a 5′ phosphate[10,11]. In addition, both RISC and RNase H–like proteins require a divalent metal ion for their activity[11]. However, in the case of RNase H, the RNA in a RNA-DNA heteroduplex is cleaved as guided by the DNA strand, whereas in RISC, the RNA in a RNA-RNA duplex is cleaved as guided by an siRNA strand. The architecture of the molecule and placement of the PAZ and PIWI domains define a groove that could be used for substrate binding. Based on the structure of PAZ with a 'mini-siRNA'[12], we modeled an siRNA binding with its 3′ end in the PAZ cleft and the siRNA-mRNA double helix extending into the groove, and suggested a mechanism for siRNA-guided mRNA cleavage[8]. The model proposing that RISC slicer activity resides in Argonaute itself was supported by mutational analysis of the conserved aspartates in human Argonaute2 (Ago2)[7]. When these were altered, the mutants lost the ability to form cleavage-competent RISC while retaining siRNA binding. This provides strong circumstantial evidence for a model in which Argonaute itself functions as the slicer enzyme in the RNAi pathway.

[1]Cold Spring Harbor Laboratory, Watson School of Biological Sciences, and [2]W.M. Keck Structural Biology Laboratory, 1 Bungtown Road, Cold Spring Harbor, New York 11724, USA. [3]These authors contributed equally to this work. Correspondence should be addressed to L.J. (leemor@cshl.edu) or G.J.H (hannon@cshl.edu).

Published online 30 March 2005; doi:10.1038/nsmb918

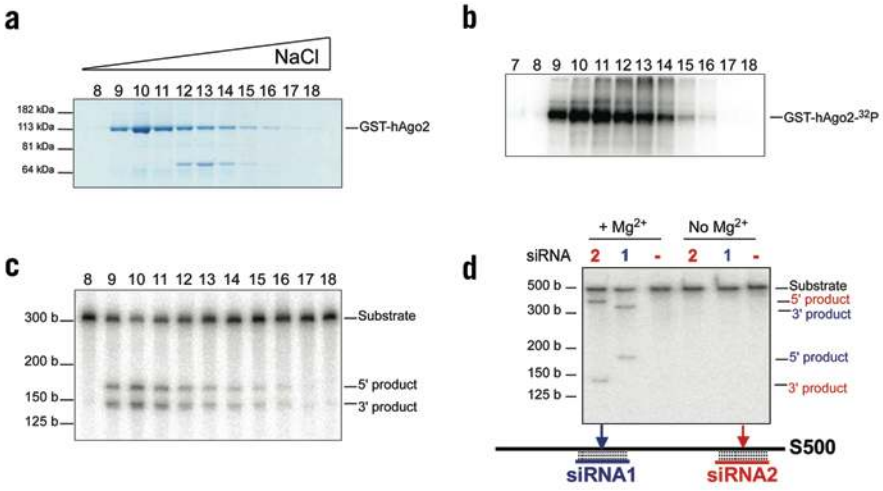

Figure 1 Ago2 and an siRNA form recombinant RISC. (**a**) Fractionation of bacterially expressed human Ago2. After affinity chromatography and size fractionation, GST-Ago2 was chromatographed on a mono Q column. Fractions from a gradient elution were electrophoresed on an SDS-PAGE gel and stained with GelCode Blue (Pierce). (**b**) Aliquots of fractions in **a** were mixed with α-^{32}P-labeled siRNA containing photoreactive dT residues in the two 3′ positions. After preincubation the mixture was irradiated with 254-nm UV light as described in Methods. Crosslinked species were resolved by SDS-PAGE. (**c**) Aliquots of fractions in **a** were mixed with a single-stranded siRNA for 30 min to permit RISC assembly. A 300-base (300-b) uniformly labeled substrate containing a sequence with perfect complementarity to the siRNA was added to the reaction. Cleavage products were resolved on a denaturing PAGE gel. (**d**) A 500-base (500-b) uniformly labeled substrate, as indicated, was mixed with recombinant Ago2 that had been charged with either of two different siRNAs, in either the presence or absence of Mg^{2+}. Cleavage products were resolved by electrophoresis and represented 5′ and 3′ fragments as indicated.

Although the aforementioned evidence is suggestive, a definitive demonstration that Argonaute catalyzes siRNA-directed cleavage can come only from biochemical reconstitution of this activity using purified components. For this reason, we sought to produce a recombinant Argonaute protein from an organism that lacks an RNAi pathway and ask whether this protein could be programmed for target cleavage by combination with an siRNA.

RESULTS

hAgo2 and an siRNA form recombinant RISC

Human Argonaute2 (hAgo2) was fused to glutathione *S*-transferase and expressed in *Escherichia coli*. A substantial fraction of the fusion protein remained soluble and could be recovered by affinity chromatography on glutathione agarose. Further fractionation of the GST-Ago2 by anion-exchange chromatography allowed the production of material that was >90% pure (for example, **Fig. 1a**, fraction 10). The identity of the GST-Ago2 protein was verified by mass spectrometry.

To probe whether bacterially expressed Ago2 retained properties of Ago2 purified from mammalian cells, we tested siRNA binding using a UV-crosslinking assay. We have previously shown that siRNAs bearing photoreactive deoxythymidine residues[13] at their 3′ ends crosslink to the PAZ domain[14], revealing an interaction that is supported by structural data[12,15]. An aliquot of each fraction from an anion-exchange column (**Fig. 1a**) was mixed with a 5′ end–labeled 21-nt siRNA containing photoreactive residues in the two 3′ positions. Whereas double-stranded siRNAs showed no ability to crosslink to recombinant Ago2 (data not shown), single-stranded siRNAs could be specifically crosslinked to the protein (**Fig. 1b**), with the relative amount of crosslinked material reflecting the abundance of the protein in each column fraction. This suggested that at least the PAZ domain was functionally intact in recombinant Ago2.

We next asked whether our recombinant Ago2 could use an siRNA as a guide for substrate cleavage. Column fractions were preincubated with a single-stranded siRNA for 30 min to permit assembly of the complex, followed by addition of a uniformly labeled, ~300-nt target. Mixtures cleaved the substrate in a manner dependent on the presence of a complementary siRNA and proportional to the amount of Ago2 in each chromatographic fraction (**Fig. 1c**,**d**). Similarly purified GST protein, lacking any Ago2 sequences, would not catalyze siRNA-directed cleavage (**Supplementary Fig. 1** online). The position of the cleavage could be shifted by changing the sequence of the siRNA provided to recombinant Ago2 (**Fig. 1d**), indicating siRNA-directed, site-specific cleavage. RISC has been shown to require metal ions for cleavage[11], and this result is in accord with the proposed catalytic mechanism of Ago2 (ref. 8). Recombinant Ago2 was completely dependent on the presence of a divalent metal for substrate cleavage (**Fig. 1d**). Recombinant RISC was competent for binding to a complementary single-stranded DNA substrate but could not cleave that target. Neither could a 21-nt single-stranded DNA direct cleavage of a complementary RNA substrate (data not shown)[7,10].

Our results indicate that a minimal RISC can be formed by the combination of recombinant Argonaute2 protein, purified from bacteria, and a synthetic, single-stranded siRNA. The availability of recombinant material allowed us to test which properties of RISC could be assigned to the Ago2–siRNA complex and which must reside in other proteins.

The siRNA 5′ phosphate stabilizes recombinant RISC

Processing of double-stranded RNAs or microRNAs by Dicer and Drosha leaves 5′-phosphate groups on the small RNAs that are assembled into RISC. This feature has been proposed as an important quality check during RISC assembly, and this function has recently been attributed to recognition of those phosphate groups within the RLC, in part by the asymmetry determining factor, R2D2 (ref. 16). It is less clear whether the siRNA 5′ phosphate plays a role within RISC itself.

To probe this question, we charged recombinant Ago2 with a 21-nt siRNA that either contained or lacked a 5′ phosphate group. We then measured the rate and extent of cleavage and the amount of recombinant RISC formed. For these assays, we used a chemically synthesized, 50-mer target labeled at its 5′ end.

Initial experiments were done with a vast excess of siRNA (100 nM, ~1,000-fold over active Ago2) to assess whether an active RISC could be assembled in the absence of a 5′ phosphate on the siRNA. Both phosphorylated and nonphosphorylated siRNAs could direct substrate cleavage (**Fig. 2a**). However, the overall amount of RISC formed was lower with the nonphosphorylated siRNA. This could be determined by comparing the extent of the pre-steady-state burst of RISC activity (**Fig. 2b** and **Supplementary Fig. 2** online). Separate incubations in the presence of [γ-^{32}P]ATP ruled out the possibility that the nonphosphorylated siRNA was being phosphorylated by a contaminating kinase in the Ago2 preparations (data not shown).

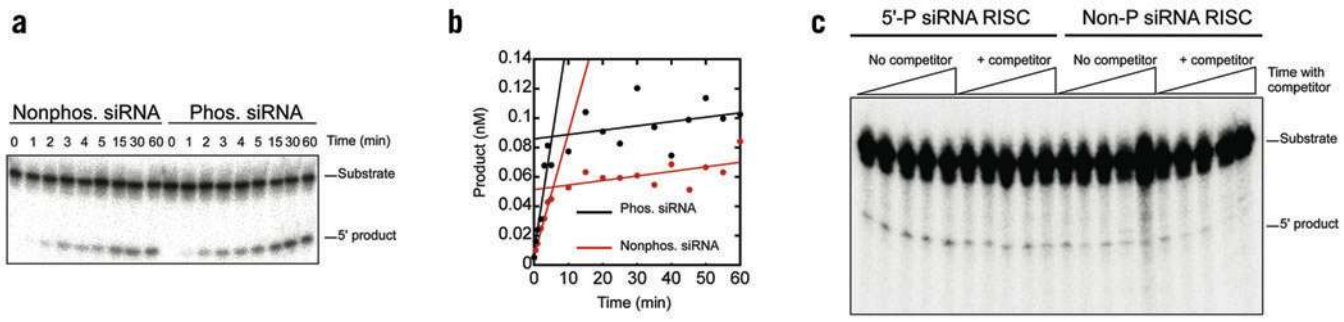

Figure 2 The 5′ phosphate contributes to the formation and stability of active RISC. (**a**) Recombinant Ago2 was charged with an siRNA containing or lacking a 5′ phosphate (as indicated). This was mixed with a 5′ end–labeled substrate consisting of a 50-nt synthetic RNA. Samples were taken at the indicated times. The position of the 5′ cleavage product is indicated. (**b**) The formation of product was quantified and plotted against reaction time. Rates were fitted using Kaleidagraph (Synergy). The initial rate of each reaction was determined from the burst and the amount of active enzyme was calculated from the *y*-intercept of the secondary phase. (**c**) Recombinant Ago2 was charged with an siRNA containing or lacking a 5′ phosphate (5′-P) for 30 min. A competitor-phosphorylated siRNA was then added and incubated for 5, 30, 60, 90 or 120 min. At the assigned time points, end-labeled substrate was added to the mixture for a 5-min cleavage reaction. The position of the 5′ cleavage product is indicated. In all cases, panels show a representative experiment of at least three independent repeats.

Although these data show an impact of the siRNA 5′ phosphate, it is clear that a phosphorylated siRNA is not absolutely required for RISC activity. We therefore examined differences in the RISCs formed with phosphorylated and nonphosphorylated siRNAs. To address the relative stability of these two complexes, we formed RISC during a 30-min assembly reaction using phosphorylated or nonphosphorylated siRNAs at 1 nM. Even at this lower siRNA concentration, ample activity could be detected using a nonphosphorylated siRNA. We then challenged each RISC with a phosphorylated competitor siRNA (100 nM) and examined RISC activity at various times after competitor addition. Whereas the RISC formed with the phosphorylated siRNA was virtually unaffected, the RISC formed with the nonphosphorylated siRNA seemed to exchange that guide for the phosphorylated competitor RNA over the time course of the experiment. This could be seen both by the loss of cleavage directed by the nonphosphorylated siRNA and by the accumulation of an activity that cleaved with the specificity of the competitor RNA (**Fig. 2c** and data not shown). Thus, the presence of the 5′ phosphate on the siRNA seems to be an important determinant of the overall stability of the Ago2–siRNA complex.

The siRNA 5′ phosphate is important for RISC fidelity

Previous studies have indicated that RISC determines its cleavage position from the 5′ end of the siRNA[17,18]. To assess whether this property was retained using bacterially expressed Ago2, the recombinant protein was incubated with siRNAs ranging from 21 to 17 nt. Each siRNA either bore or lacked a 5′ phosphate group. To create the shorter siRNAs, we removed sequences from either the 5′ end or the 3′ end of the 21-mer. When the phosphorylated siRNA was truncated from its 3′ end, we saw cleavage with all three siRNAs, the 21-mer, the 19-mer and the 17-mer, to similar degrees (**Fig. 3a**). As expected, the position of cleavage did not shift. Furthermore, the size of the product is as expected for cleavage of the substrate between the nucleotides complementary to bases 10 and 11 of the siRNA. The siRNAs that lacked 5′ phosphates showed a similar pattern of activity, except that, particularly with the shortest siRNA, we noted reduced activity in the absence of phosphate.

Truncation of the siRNA from the 5′ end resulted in cleavage at a site that shifted within the substrate by precisely the number of bases removed from the siRNA. This is again consistent with Ago2 determining the cleavage position by reference to the 5′ end of the siRNA.

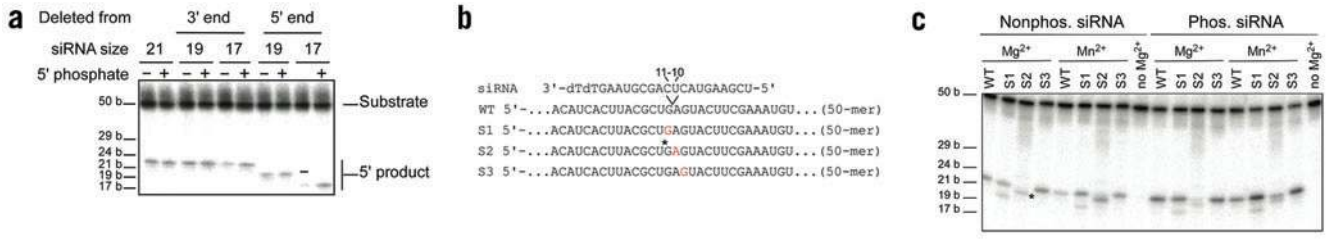

Figure 3 Cleavage by recombinant RISC is accurate. (**a**) siRNAs either bearing or lacking 5′ phosphates (as indicated) were used to reconstitute RISC with recombinant hAgo2. Sequences were removed from either the 5′ or 3′ end to create shorter siRNAs of the indicated lengths. Positions of the substrate and the 5′ product are shown. Products were analyzed on 20% (w/v) PAGE gels. b, base. (**b**) Synthetic substrates used in **c** are shown along with the siRNA used to reconstitute RISC. The predicted cleavage position is indicated by the arrow. Red nucleotides denote the position of the phosphorothioate as being 5′ to the highlighted position. Asterisk, observed position of cleavage of S2 in the absence of the 5′ phosphate on the siRNA. (**c**) Phosphorylated or nonphosphorylated siRNA of the sequence in **b** was used to program recombinant Ago2. This was reacted with the indicated substrate in the presence of Mg^{2+} or Mn^{2+} or in the absence of divalent metal. Positions of the substrate and 5′ product are indicated. Asterisk denotes inaccurate cleavage of S2 in the absence of the siRNA 5′ phosphate. Gels shown are representative of at least three independent repeats. b, base. WT, wild type.

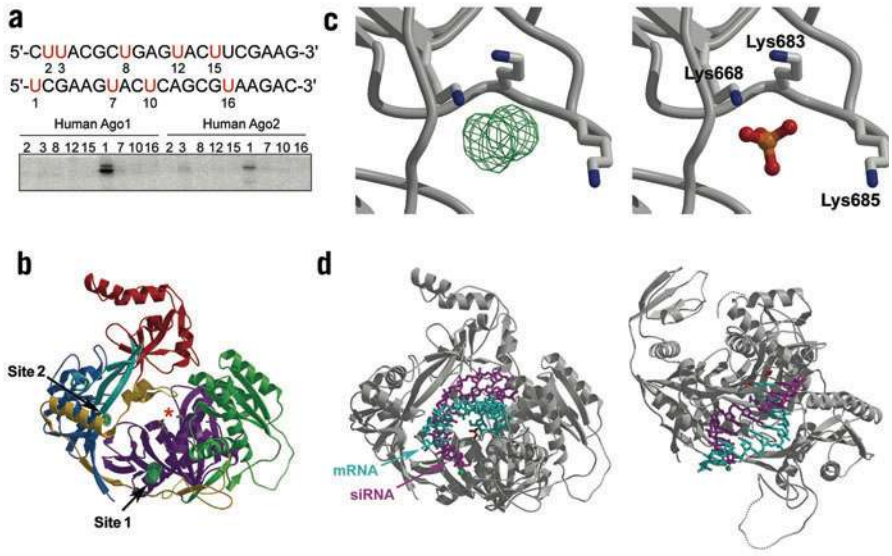

Figure 4 Position of the 5′ end of the siRNA in RISC. (**a**) siRNAs derivatized with iodouridine at selected positions (red) were mixed with 293 cell extracts containing epitope tagged human Ago1 or Ago2. After UV irradiation, crosslinked species were recovered by immunoprecipitation and resolved by gel electrophoresis. (**b**) Ribbon representation of PfAgo showing the N-terminal domain (blue), the stalk (light blue), the PAZ domain (red), the middle domain (green), the PIWI domain (purple), and the interdomain connector (yellow). The molecule is shown from one end of the groove toward the active site (marked by a red asterisk). The active site aspartates are in stick representation. Disordered loops are dotted lines. The difference Fourier electron density map contoured at 5 σ (aquamarine) shows the tungstate-binding sites. Site 1 is a double peak shown in the front at one end of the binding site groove leading to the active site. Site 2 is nestled between the stalk and the interdomain connector and less accessible to an oligonucleotide. (**c**) $F_o - F_c$ electron density map (left) contoured at 5 σ around tungstate-binding site 1. The double peak indicates two close tungstate positions (see text). A tungstate ion modeled into the density (right) with tungsten in orange and oxygen in red (only one is shown for clarity). Three lysines, two of which reside on the PIWI box, form a positively charged pocket suitable for phosphate binding. (**d**) An A-form RNA decamer duplex was placed in the main groove of PfAgo with the 5′ end of the siRNA (purple) near the tungstate-binding site 1 (aquamarine sphere) (see text and Methods). The scissile phosphate on the target mRNA (light blue) is at a position opposite to the phosphate between nucleotides 10 and 11 of the siRNA. In this model, this phosphate falls near the active site aspartates (red). The view on the left is identical to the view in; the view on the right is rotated ~60° around the horizontal axis.

To examine the fidelity of our recombinant, minimal RISC, we turned to the observation that replacement of the scissile phosphate with a phosphorothioate prevents Mg^{2+}-catalyzed RISC cleavage[11]. We synthesized three additional 50-mer targets, each with a single phosphorothioate substitution (**Fig. 3b**). Substrate S1 contains the substitution in the bond one position in the 5′ direction of the predicted cleavage site, whereas S3 contains the substitution one position in the 3′ direction of the predicted cleavage site. Substrate S2 has the substitution at the cleavage site itself.

Ago2 was primed with a phosphorylated siRNA and reacted with the wild-type or modified substrate RNAs in the presence of Mg^{2+}. The fidelity of the minimal RISC is indicated by its essential inactivity toward the S2 substrate, whereas cleavage of S1 and S3 remained strong (**Fig. 3c**). It has previously been shown that Mn^{2+} could partially rescue the effects of phosphorothioate substitution, consistent with its stronger interaction with the sulfur group[11]. Substitution of Mg^{2+} with Mn^{2+} in our recombinant RISC also partially rescued cleavage of the S2 substrate. Ca^{2+} had no effect on protein-catalyzed cleavage (data not shown).

Somewhat different results were seen with the nonphosphorylated siRNA. Cleavage of the wild-type, S1 or S3 substrate was not altered by the absence of the phosphate. However, cleavage of S2 was relatively efficient but was shifted one base in the 5′ direction of its normal position. Addition of Mn^{2+} to RISC did not substantially alter the cleavage pattern, with the position remaining shifted by one base relative to the normal site.

These results indicate that the minimal RISC formed from recombinant Ago2 and a single-stranded siRNA is accurate. Notably, the 5′ phosphate of the siRNA had an impact on the fidelity of the enzyme, particularly under conditions in which the normal cleavage site becomes unavailable. In the absence of the 5′ phosphate, the siRNA seems to be able to slide within the enzyme, permitting an altered positioning of phosphate groups on the target with respect to the active site. Thus, the 5′ phosphate group on the siRNA plays multiple roles within RISC, contributing to the binding of the siRNA by Ago2 and ensuring the correct positioning of the siRNA within the enzyme. We therefore sought the position of the 5′ phosphate within the enzyme.

Argonaute recognizes the 5′ end of the siRNA

We synthesized a series of siRNAs that were modified to contain photoreactive residues at defined positions. Substitutions of 5-iodouridine for uridine were made at selected positions within the first 16 nt of the siRNA (**Fig. 4a**, red). These siRNAs were labeled at their 5′ ends and used to assemble RISC in extracts from 293 cells that stably express epitope-tagged human Argonaute proteins. After irradiation, Ago1 or Ago2 was recovered by immunoprecipitation. As we have previously shown, both Ago1 and Ago2 can be crosslinked to siRNAs through an interaction between the PAZ domain and the siRNA 3′ end[14]. Similarly, both Argonaute proteins can be crosslinked to siRNAs with photoreactive residues in position 1 but not to siRNAs with photoreactive residues in several other positions (**Fig. 4a**). These results do not rule out the possibility that internal positions are in close contact with Ago2, as an aromatic residue within the protein needs to be available for formation of the crosslink. However, they are consistent with the model that Ago2 engages the 5′ end of the siRNA at a position within the protein that determines the cleavage site. The aforementioned data suggests that this interaction involves the 5′ phosphate on the siRNA but also indicates other modes of interactions, probably binding of the 5′ base or phosphate backbone.

To locate the 5′ end of the siRNA within Argonaute, we took advantage of our previous structural studies of PfAgo[8]. We reasoned that we might be able to locate a possible phosphate-binding site by soaking crystals of PfAgo with a tungstate salt. Tungstate (WO_4^{2-}) is similar to phosphate (PO_4^{2-}) and could potentially bind to a phosphate-binding site[19,20]. Even though the RNA backbone contains many phosphate groups, the

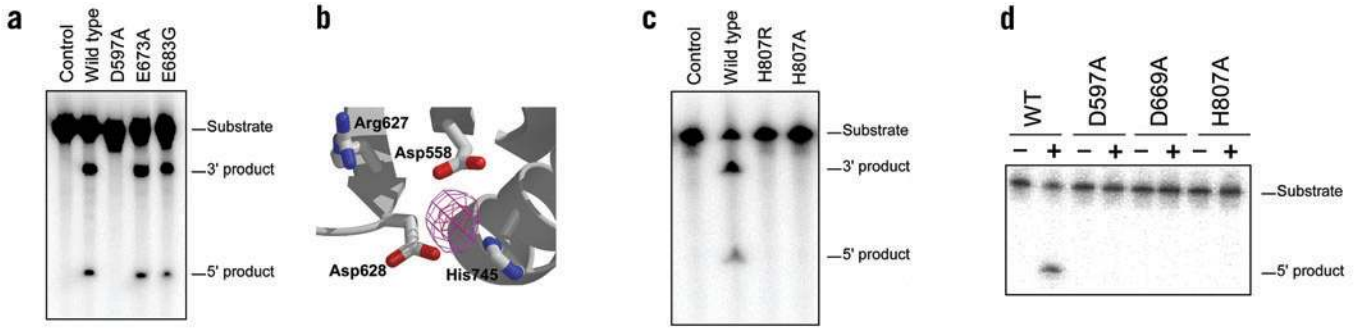

Figure 5 The catalytic site of Ago2. (**a**) Constructs of hAgo mutant proteins were prepared by site-directed mutagenesis in which putative catalytic residues were changed to alanine or glycine, as indicated. These were cotransfected into human 293 cells with an siRNA-targeting firefly luciferase. RISC was immunoprecipitated from these cells and tested for activity against a complementary substrate. Positions of the 5′ and 3′ cleavage products are indicated. (**b**) $F_o - F_c$ electron density map, contoured at 5 and 8 σ (pink and red) clearly shows the location of the Mn^{2+} ion in the PfAgo–Mn^{2+} complex coordinated to the two aspartates previously implicated as well as His745. Glu635 (see **Fig. 6**) is on the other side of the active site. (**c**) Constructs were prepared that direct the expression of hAgo2 in which the putative active site histidine (His807) was mutated to arginine or alanine. This was cotransfected into human 293 cells along with an siRNA targeting luciferase. RISC was recovered as in **a** and tested for activity. Positions of the 5′ and 3′ cleavage products are indicated. (**d**) Bacterially expressed hAgo2 proteins containing the indicated mutations were purified. These were tested for cleavage activity against the 5′ end–labeled 50-nt synthetic RNA substrate in the absence (–) and presence (+) of a complementary siRNA. Positions of the substrate and 5′ cleavage product are indicated.

terminal phosphate is unique in charge and is unbound on one side. Therefore, we expect that a tungstate ion would preferentially bind to the terminal phosphate-binding site. In addition, tungsten is substantially heavier than phosphorous, has more electrons, and produces an anomalous signal. We therefore anticipated that the position of this metal could be easily identified crystallographically.

Native PfAgo crystals were soaked with Na_2WO_4 and data were collected at the tungsten peak wavelength to a resolution of 2.5 Å (see Methods). Anomalous difference Fourier and $F_o - F_c$ electron density maps showed two strong peaks (>45 σ for the anomalous difference, and >5 σ for the Fourier difference) (**Fig. 4b**). One is nestled between the stalk and the interdomain connector, away from the groove and not very accessible to an oligonucleotide (site 2) (**Supplementary Fig. 3** online). The other appears as a double peak, and we therefore placed two tungstates, with 0.5 occupancy each, in this site (site 1). This double peak is in a notable position because of its location on the end of a long, positively charged groove on the opposite side from the PAZ domain cleft. We previously suggested that this basic groove could be suitable for siRNA and mRNA-substrate binding with the 5′ end of the siRNA projecting toward the portion of the molecule containing site 1 (ref. 8). The tungstates in site 1 interact with several lysines from the PIWI domain, two of which reside in a relatively conserved region of the PIWI domain known as the PIWI box[21] (**Fig. 4c**). These lysines are not strictly invariant in other Argonaute proteins, but several lysine, arginine and other phosphate-binding residues are present in that region in other Ago proteins.

To examine whether site 1 falls in a position appropriate for binding the 5′ phosphate of the siRNA, we modeled an A-form RNA duplex in this portion of the groove (**Fig. 4d**). We placed the 5′ phosphate of the strand defined as the siRNA in site 1. The other strand would be regarded as the mRNA substrate. To permit this placement of the RNA, two loops of PfAgo, one of which leads to a disordered region, had to be moved, but no adjustments had to be made to the RNA. According to this model, the phosphate between nucleotides 10 and 11 from the 3′ end of the 'mRNA' would fall very near the active site residues and precisely at the position of mRNA cleavage by RISC[17,18]. The details of the interaction, the fine structure of the RNA, and its precise docking on the protein all await a cocrystal structure of Argonaute with RNA. Nonetheless, the tungstate-binding site 1 near the PIWI box is consistent with a possible location for the 5′ phosphate of the siRNA with an appropriate distance from the active site.

A previous study[9] suggested a different site as a putative 5′-phosphate-binding site. This is located at or near a metal-binding site, in which the metal is coordinated by the C terminus of AfPiwi. An analogous site does not seem to coordinate a metal ion in PfAgo. This region is a positively charged pocket, conserved in both AfPiwi and PfAgo. In PfAgo this pocket is internal in a long positively charged groove, and in our model the region would be proposed as a binding site for an internal backbone phosphate of an RNA. The tungstate-binding site, which we suggest to be the 5′-phosphate-binding site, is at one end of this long groove.

A unique DDH motif comprises the active site of Argonaute

RNase H–related enzymes, such as RNase H1, RNase HII, transposases and integrases, contain three highly conserved carboxylates, which make up an Asp-Asp-Glu (DDE) motif[22]. The position of the two aspartates is always similar but the third carboxylate, a glutamate, varies in its position within the active site. Previously, we located two aspartates in the positions similar to those found in other RNase H family enzymes[8]. These two conserved active site aspartates in hAgo2 were mutated to alanine, and the resulting proteins were incapable of assembling into a cleavage-competent RISC *in vitro* or *in vivo*[7]. We also noted a glutamate in close proximity to the two aspartates in the PfAgo structure. This glutamate can be aligned with conserved Glu683 in hAgo2. However, owing to an insertion in the sequence of the mammalian Argonaute proteins relative to PfAgo, it could alternatively align with another conserved glutamate in hAgo2, Glu673. To determine whether either of these glutamates was the third residue of the catalytic triad, each was changed to alanine in hAgo2. Notably, both mutants retained slicer activity (**Fig. 5a**).

RISC and RNase H enzymes require a divalent metal ion for catalysis[11,22]. To aid in location of the third catalytic residue, we soaked PfAgo crystals with $MnCl_2$ and collected data to a resolution of 2.7 Å (**Table 2**). Mn^{2+} was chosen as it can replace Mg^{2+} in RISC but is heavier and easier to locate crystallographically. A difference Fourier electron density map ($F_o - F_c$ using phases calculated from the native PfAgo structure without solvent atoms) showed a strong 10 σ peak at the active site marking the location of the Mn^{2+} ion (**Fig. 5b** and **Supplementary Fig. 4** online).

As we anticipated, we found that the metal was coordinated to the two aspartates; however, it was also coordinated to a histidine, impli-

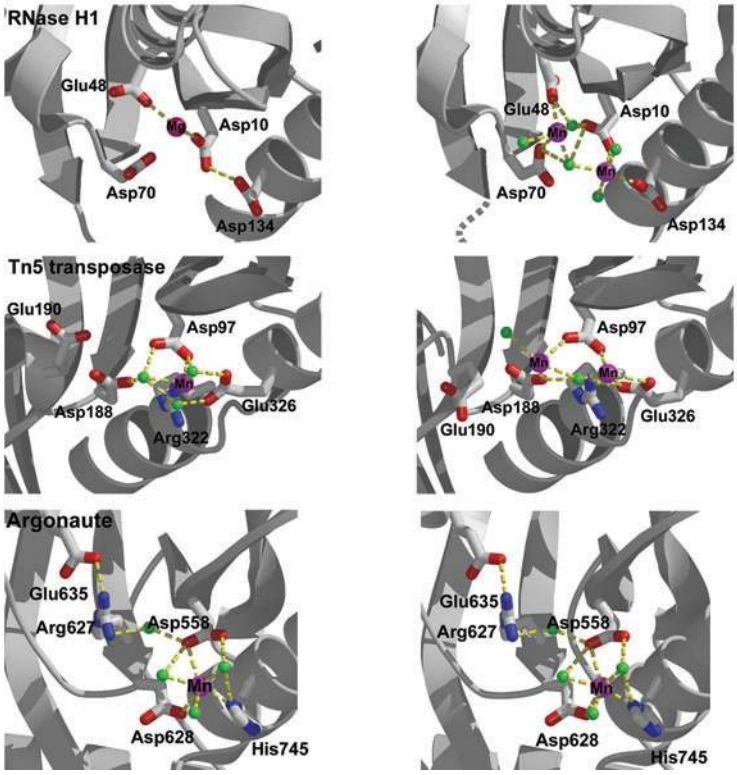

Figure 6 Comparison of active sites in RNase H–fold proteins. The active sites of *E. coli* RNase H1 (top), Tn5 transposase (middle) and PfAgo (bottom in stereo) showing one or two metal ions binding. A ribbon diagram is shown for the proteins with the active site residues discussed in stick representation. Mg^{2+} ions are drawn as dark pink and Mn^{2+} ions as magenta spheres. For RNase H1, a Mg^{2+} ion is coordinated to an aspartate and a glutamate of the DDE motif in the one-metal binding structure[30] (PDB entry 1RDD). Two Mn^{2+} ions are bound, one to the primary site to the DDE motif, and a second to one of these aspartates and an additional aspartate in what is considered an inhibitory site[29] (PDB entry 1G15). The Mn^{2+} ions in Tn5 are bound to the DDE motif, with the location of the glutamate on the opposite side of the aspartates compared to RNase H1 (refs. 34,36; PDB entries 1MUR and 1MM8). The DNA substrates that are bound in both Tn5 structures were removed for clarity, however, they participate in metal coordination as well. The Mn^{2+} ion in the PfAgo–Mn^{2+} complex, shown on the bottom, coordinates to the side chains of the DDH motif (this work). Note that the histidine is in a similar position to the DDE glutamate of Tn5. Another glutamate is located on the other side of the aspartates in Tn5 and in PfAgo, neither of which appear to participate in metal coordination.

cating it as the third catalytic residue (**Fig. 5b**). Examination of the sequence alignment of PIWI domains revealed that the histidine is conserved in hAgo2 and hAgo3, but is an arginine in inactive Argonautes hAgo1 and hAgo4. We therefore changed the corresponding residue in hAgo2, His807, to alanine and to arginine. In both cases, mutation abolished the mRNA cleavage activity of enzymes assembled *in vivo* (**Fig. 5c**). Mutations of active site aspartates and the histidine were also introduced into bacterially expressed recombinant hAgo2. As expected, none of the three mutants cleaved substrate (**Fig. 5d**), although each could be crosslinked to photoreactive siRNAs (data not shown).

Thus, it seems that in contrast to RNase H–fold enzymes such as RNase H, transposases and integrases, which all have active site DDE motifs, Argonaute uses a unique DDH motif for metal ion coordination. The precise role of the metal ions in these enzymes remains somewhat unclear. Both one- and two-metal ion mechanisms have been proposed for RNase H–type enzymes[23–25]. *E. coli* RNase H1 is thought to work via a one-metal ion mechanism in which Mg^{2+}, coordinated by two carboxylate groups, mediates interactions with the nucleic acid substrate. The other carboxylate anchors a water molecule, which can act as a general acid[24,26]. The two-metal ion mechanism was first proposed for the 3′→5′ exonuclease of the Klenow fragment[27,28]. In this case, one metal interacts with the substrate and stabilizes the reaction intermediate while the other activates a water molecule and positions it to attack the scissile phosphate. Both one and two metal ions have been observed in crystal structures of *E. coli* RNase H1 (refs. 29,30), one in the case of *A. fulgidus* RNase HII[31] and two in the active site of the isolated HIV RNase H domain of reverse transcriptase[23]. The absence of a second metal ion in a crystal structure does not preclude a two-metal ion mechanism, as the second metal may have weak binding in the absence of substrates. However, there are indications that RNase H1 uses a single-metal ion mechanism, whereas HIV reverse transcriptase RNase H uses two[32]. In fact, the second metal ion may even be inhibitory in RNase H1 (ref. 32). The best-characterized system is probably that of Tn5 transposase, where several structures exist of protein–DNA complexes, and these can be rationalized with extensive biochemical and mutagenesis studies (reviewed in ref. 33). Tn5 transposase uses a two-metal ion mecha-

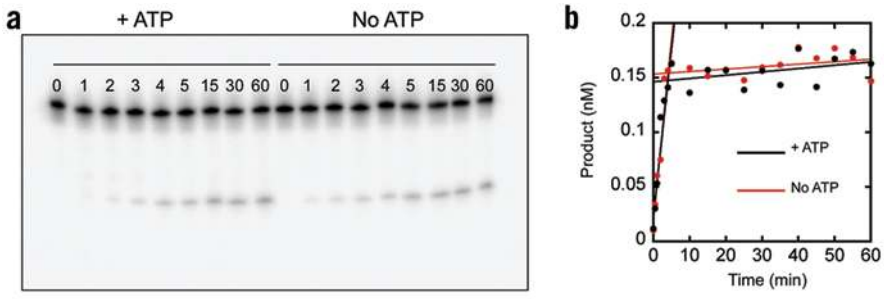

Figure 7 ATP does not accelerate cleavage by recombinant RISC. (**a**) Recombinant RISC was prepared by incubation of a 5′-phosphorylated siRNA and bacterially expressed hAgo2. After a 30-min preincubation, this was mixed with a complementary target and product formation was followed over time in the presence or absence of ATP. (**b**) Product formation was plotted against time for reactions in the absence (red) or presence (black) of ATP. The *y*-intercept of the secondary rate indicates the concentration of active enzyme. Panels are representative of at least three independent experiments.

nism for its activity. Structures are available with substrate and either one[34] or two Mn^{2+} ions[35,36] in the active site. The first Mn^{2+} ion is coordinated by Glu326, Asp97, the 3′ OH of the transferred strand and a water molecule. The second Mn^{2+} ion is coordinated to Asp97, Asp188, an oxygen of the 5′ phosphate of the nontransferred strand and two water molecules. Both metal ions are also bridged by an oxygen of the 5′ phosphate.

The location of the two aspartates of the DDE or DDH motif is identical in *E. coli* RNase H1, Tn5 transposase and PfAgo (**Fig. 6**). However, the Mg^{2+} in the primary metal-binding site of RNase H1 is coordinated to a glutamate on one side of the active site, whereas Mn^{2+} in Tn5 and in PfAgo is coordinated to either a glutamate (for Tn5) or a histidine (for PfAgo) on the other side of the active site. The Tn5 glutamate and the PfAgo histidine are located in similar positions. RNase H1 has an aspartate at that position, which binds the second, possibly inhibitory, metal ion. Avian sarcoma virus integrase with a similar fold and nearly identical configuration of the DDE motif also shows binding of two metal ions[37]. Both Tn5 and PfAgo also have glutamates on the opposite side of the active site, which do not seem to participate in metal coordination. Notably, an E326D substitution in Tn5 results in a more efficient enzyme[38]. Thus the similarities of PfAgo to Tn5 transposase are especially marked.

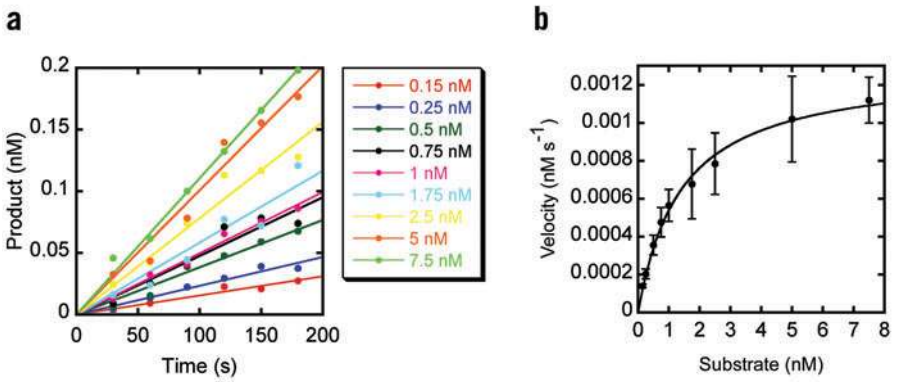

Figure 8 Kinetic analysis of recombinant RISC. (**a**) The initial velocity of recombinant RISC was plotted by monitoring product formation versus time at different substrate concentrations. (**b**) Plotting initial velocity versus substrate concentration permits calculation of K_m and V_{max} for the reconstituted enzyme (see text).

Recombinant RISC lacks ATP-assisted product release

RISC assembled in *D. melanogaster* extracts uses ATP hydrolysis to accelerate product release and thus permit rapid, multiple cycles of substrate cleavage[39]. We sought to determine whether our minimal, recombinant RISC also carried out multiple cycles of product cleavage and whether this was enhanced by ATP. Measuring the rate of product formation over time did not reveal any effect of ATP in the recombinant system (**Fig. 7a**,**b** and **Supplementary Fig. 5** online), strongly suggesting that a protein other than Ago2 uses the energy of ATP hydrolysis to facilitate product release in a more complete RISC formed *in vivo*.

We examined the kinetic properties of our enzyme by measuring the K_m, V_{max} and k_{cat} of the Ago2–siRNA complex (**Fig. 8**, **Table 1** and **Supplementary Fig. 6** online). Previous studies have indicated a K_m for *D. melanogaster* RISC measured with a perfectly complementary siRNA of ~8.4 nM (ref. 39), whereas human RISC affinity selected from extracts showed a K_m of ~2.3 nM (ref. 10). Using recombinant hAgo2 and a different siRNA, we arrive at a markedly similar K_m value of ~1.40 nM. Additionally, the *D. melanogaster* enzyme showed a V_{max} at 1 nM enzyme of 7.1 pmol s^{-1} and human RISC showed a V_{max} of ~7 pmol s^{-1} at 0.4 nM RISC[10,39]. Recombinant human RISC showed a very similar maximal velocity of 1.30 pmol s^{-1} at 0.15 nM RISC. This gives k_{cat} values for the *D. melanogaster* and recombinant human enzymes of 7.1×10^{-3} and 17.9×10^{-3} s^{-1}, respectively. The k_{cat} of the recombinant enzyme was calculated as 8.7×10^{-3} s^{-1}. The agreement between these parameters shows that recombinant RISC and the more complete complexes formed in extracts are very similar enzymes, with the implication that Ago2 and the siRNA are not normally assisted by other proteins, such as factors that remodel or activate the complex, for substrate binding and cleavage.

Table 1 Kinetic parameters

	Recombinant RISC	*D. melanogaster* RISC[39]	Human RISC[10]
K_m (nM)	1.40 ± 0.12	8.4 ± 1.6	2.3 ± 0.3
V_{max} (nM s^{-1})	0.00130 ± 0.00004	0.0071	0.0071 ± 0.0003
[Enzyme] (nM)	0.150 ± 0.05	1	0.4
k_{cat} (s^{-1})	8.7×10^{-3}	7.1×10^{-3}	17.9×10^{-3}
k_{cat} K_m^{-1} (nM^{-1} s^{-1})	6.2×10^{-3}	0.9×10^{-3}	7.8×10^{-3}

DISCUSSION

The results presented here unequivocally demonstrate that Argonaute and a single-stranded siRNA together form a recombinant minimal RISC that can accurately cleave substrate RNAs. With the availability of this recombinant complex, we were able to test characteristic features of RISC and assign these properties to Ago2 or to other proteins in the RNAi pathway. Kinetic studies indicate that Ago2 and the siRNA form a multiple-turnover enzyme with kinetic properties that resemble, in the absence of ATP, the RISC formed in *D. melanogaster* or human cell extracts. However, our data strongly indicate that ATP-assisted product release is carried out by another, yet to be identified factor. This observation is not surprising to us considering that structural analysis of archaeal Argonaute proteins did not reveal a site predicted to bind and hydrolyze ATP. Several candidates have been identified that could potentially serve as ATP-dependent release factors in genetic and biochemical studies of RNAi. Prominent among the candidates are RNA helicases, such as dmp68, that interact physically with *D. melanogaster* Argonaute2, and other helicases that have been linked to the RNAi pathway through genetics[40–44].

Many studies have suggested that the 5′ phosphate of the siRNA 'licenses' small RNAs for entry into the RNAi pathway[45]. Our results suggest that the majority of discrimination does not occur within the Ago2–siRNA complex itself. Instead, the presence of the phosphate contributes to the stability of the Ago2–siRNA complex and to the fidelity with which this enzyme cleaves its substrates.

Consistent with previous reports, our results indicate that Ago2 measures from the 5′ end of the siRNA to determine the cleavage site within the target[45]. Using the *P. furiosus* protein as a model system for

Table 2 Data collection and refinement statistics

	Mn^{2+}	Tungstate
Data collection		
Space group	$P2_1$	$P2_1$
Cell dimensions		
a, *b*, *c* (Å)	68.7, 105.1, 73.66	69.1, 103.51, 73.25
α, β, γ (°)	90, 102.70, 90	90, 102.47, 90
Resolution (Å)	50-2.7 (2.8–2.7)	50-2.5 (2.59–2.50)
R_{sym}	0.093 (0.520)	0.065 (0.505)
$I / \sigma(I)$	26.4 (3.7)	22.9 (3.2)
Completeness (%)	99.6 (100)	98.7 (98.8)
Redundancy	4.0 (4.2)	6.6 (6.5)
Refinement		
Resolution (Å)	50–2.7	50–2.5
No. reflections	26,404	32,350
R_{work} / R_{free}	0.215 / 0.274	0.224 / 0.282
No. atoms		
Protein	5920	5951
Ligand/ion	1	3 (W), 12 (O)
Water	165	140
B-factors		
Protein	57.86	70.58
Ligand/ion	44.56	69.74
Water	47.89	58.26
R.m.s. deviations		
Bond lengths (Å)	0.0071	0.0069
Bond angles (°)	1.314	1.382

structural studies, we located a potential binding site for the 5′ phosphate of the siRNA within RISC by identifying binding sites for a phosphate analog, tungstate. Of the two binding sites identified, one was in a position that is predicted to be accessible to the siRNA-target duplex. Modeling studies suggest that if the siRNA 5′ phosphate were engaged in this position within the protein, an A-form RNA helix between the siRNA and the substrate would bring the scissile phosphate into close proximity with the active site of the enzyme.

Through a combination of structural studies and genetic analysis, we have produced a refined model of the RISC active site. We previously predicted a potential Ago2 catalytic site glutamate by analogy to other RNase H family proteins[7,8]. Notably, mutation of two possible glutamates had no effect on Ago2 slicer activity. A resolution to this puzzle came from studies of PfAgo crystals that had incorporated a Mn^{2+} ion. This metal was engaged by the previously validated active site aspartates, as well as a histidine residue that is also conserved in human Ago2. Mutation of these residues inactived slicer in both complexes formed *in vivo* and in the recombinant protein. The arrangement of the active site in this fashion strengthens the structural relationship between Argonaute proteins and transposase and integrase family proteins, although Argonautes are unique in their use of a histidine rather than a carboxylate. Of the four human Argonaute family proteins, only one is catalytically competent[6,7]. The inactivity of Ago4 can be explained by the absence of a crucial aspartate. The finding of histidine as the third catalytic residue now explains the inactivity of Ago1, leaving only the catalytic defect in Ago3 unexplained at the structural level.

The results presented here pave the way for building toward a recombinant RISC complex that recapitulates all of the activities that have been assigned to RISC formed *in vivo*. The availability of recombinant, minimal RISC also provides a foundation for structural studies of a catalytically active complex that may reveal intricacies of RNAi biochemistry that cannot be intuited from current models.

METHODS

Oligonucleotide synthesis and modifications. All oligos used were obtained from Dharmacon. The sequence of the 50-mer target RNA was 5′-GAGGUGGACA UCACUUACGC UGAGUACUUC GAAAUGUCCG UUCGGUUGGC. Where appropriate, the oligos were 5′-phosphorylated, either with [γ-^{32}P]ATP (NEN) or unlabeled ATP (Roche). In all cases, 50-mer oligos used as targets for cleavage assays were gel-purified after end-labeling with [γ-^{32}P]ATP as described[46]. Where specified, capped, uniformly radiolabeled Luciferase targets (either 300 or 500 bp in length) were used in cleavage assays.

Sequences of siRNAs used for cleavage assays and dTdT photocrosslinking were as follows: 21-mer, 5′-UCGAAGUACUCAGCGUAAGdTdT; 3′ 19-mer, 5′-UCGAAGUACUCAGCGUAdTdT; 3′ 17-mer, 5′-UCGAAGUACUCAGCGdTdT; 5′ 19-mer, 5′-GAAGUACUCA GCGUAAGdTdT; 5′ 17-mer, 5′-AGUACUCAGC GUAAGdTdT; 5′ 29-mer, 5′-CGGACAUUUCGAAGUACUCAGCGUAAGdTdT; 5′ 24-mer, 5′-AUUUCGAAGUACUCAGCGUAAGdTdT.

Protein expression and purification. Full-length human Argonaute2 protein (GenBank entry NP_036286) was expressed as a GST fusion in *E. coli* BL21-RIPL-NT9 (derived from BL21-RIPL cells from Stratagene harboring a pET28 plasmid that directs expression of HSP90). After growth to A_{600} of 0.6 at 37 °C, cells were induced with 1 mM IPTG and grown overnight at 25 °C. Cells were lysed by sonication in 500 mM NaCl, 50 mM Tris-HCl buffer, pH 8.0, and supplemented with complete protease inhibitor cocktail (Roche). GST-Ago2 was purified using a glutathione agarose column (Sigma) using 15 mM reduced glutathione in lysis buffer, gel filtration using a Superdex 200 column (Amersham) and anion exchange on a Mono Q column (Amersham) using a 0–1 M NaCl gradient in 50 mM Tris, pH 8.0. Single-residue mutations were introduced in hAgo2 by QuikChange (Stratagene) and the mutants expressed and purified as described above.

mRNA cleavage assay. mRNA cleavage assays were done as described[7,8] using 0.125 μg of recombinant hAgo2. For reconstitution of RISC activity, 2 μl of 1 μM single-stranded, phosphorylated siRNA (not phosphorylated when indicated) were added, and the mixture was incubated at 37 °C for 30 min, followed by addition of mRNA target. Final volume of all reactions was adjusted to 20 μl after addition of target. For a standard cleavage assay, reactions were stopped after 1 h by addition of TRIZOL, followed by RNA extraction and PAGE analysis. For kinetic assays, cleavage reactions were carried out at 42 °C for the indicated times. When done under 'no ATP' conditions, reactions lacked ATP, GTP and the regeneration system. When indicated, $MgCl_2$ was excluded or replaced by 2mM $MnCl_2$ as needed. For siRNA competition experiments, recombinant hAgo2 (0.125 μg) was charged with an siRNA (1 nM) containing or lacking a 5′ phosphate for 30 min at 37 °C. A competitor-phosphorylated siRNA (100 nM) was then added and incubated for 5, 30, 60, 90 or 120 min. Target was added at the designated times for a 5-min cleavage reaction at 42 °C. Cleavage products were analyzed as described above.

UV photocrosslinking. UV photocrosslinking of dTdT-containing oligos to Argonaute protein, either in immunoprecipitates or with recombinant hAgo2, was done as described[7,8]. Briefly, reactions were assembled as in mRNA cleavage assays except that no target was added, and the siRNA was 5' end–labeled. Reactions were UV crosslinked (254 nM) for 10 min, followed by SDS-PAGE analysis. UV photocrosslinking of siRNAs modified with 5-iodo uridine was similarly done, except that the crosslinking wavelength used was 312 nm. The concentration of the crosslinking oligo was ~2 nM. When comparing different siRNAs, similar amounts of siRNA were end-labeled, and a comparable amount of counts were used in each crosslinking reaction.

Creation of 293S cell line stably expressing Argonaute2. Human 293S cells were transfected with myc-tagged Argonaute1 or 2 constructs using Transit-Lt1 reagent (Mirus) as described[7]. Transfected cells were then passaged in medium containing 500 μg ml^{-1} G418 (Roche) for selection of stable transfectants. Cell lysis and immunoprecipitation of myc-tagged Ago1 or 2 for photocrosslinking analysis was done as described[7].

Data collection and refinement. For the tungstate complex, native PfAgo crystals[8] were soaked in 20 mM Na_2WO_4, 50 mM Tris-HCl, pH 8.0, 100 mM NaCl, 7% (v/v)1-butanol, 10% (v/v) ethylene glycol for 3 h. For the manganese complex, native PfAgo crystals were soaked in 25 mM $MnCl_2$, 50 mM Tris-HCl, pH 8.0, 100 mM NaCl, 7% (v/v)1-butanol, 10% (v/v) ethylene glycol for 3 h. For cryoprotection, both crystals were soaked for 1 min in the soak solution containing increasing amounts of ethylene glycol in 5% steps to a final ethylene glycol concentration of 40% (v/v). Data were collected at a wavelength of 1.2139 Å for the tungstate complex, where anomalous signal of *W* is the strongest to a resolution of 2.5 Å. For the manganese complex, data were collected at 1.1 Å to a resolution of 2.7 Å. In both cases, data were collected under cryogenic conditions (100 K) at beamline X26C at the National Synchrotron Light Source at Brookhaven National Laboratory. Data were processed with HKL2000 (ref. 47), model building was done with O[48], and refinement with CNS[49]. For the PfAgo–Mn^{2+} complex, 83.8% and 16.2% of residues were in core and allowed regions, respectively, of the Ramachandran plot, and for the tungstate complex, 84.7% and 15.3%. For data collection and refinement statistics see **Table 2**.

Model building. A ten-base pair double-stranded RNA (dsRNA) molecule taken from the structure of the dsRNA-binding domain from *Xenopus laevis* RNA-binding protein A in complex with dsRNA[50] (PDB entry 1DI2) was docked into the groove of PfAgo while placing the 5′ phosphate of one strand on the tungstate-binding site we denote as the putative 5′-phosphate-binding site for the siRNA. Two loops from the protein, residues 282–291 and 688–691, were removed. They are not involved in any crystal contacts and although the region N-terminal to the first loop is disordered, the *B*-factors of these loops are not particularly high (~30 Å^2). However, upon a possible opening of the groove to allow substrate binding we assume that they would move. No energy minimization was done and no adjustment to the A-form RNA was made, indicating that the fit was achieved even with simple docking.

Figures. Figures 4b–d, **5b** and **6** were prepared with BobScript[51] and Raster3D[52,53].

Coordinates. The atomic coordinates and structure factors of the PfAgo–Mn^{2+} and PfAgo–tungstate complexes have been deposited in the Protein Data Bank (accession codes 1Z25 and 1Z26, respectively).

Note: Supplementary information is available on the Nature Structural & Molecular Biology website.

ACKNOWLEDGMENTS

We thank members of the Hannon and Joshua-Tor laboratories for helpful discussions and A. Heroux (X26C) for support with data collection at the National Synchrotron Light Source (NSLS). C. Marsden and S. Smith provided technical support. P. Zamore kindly provided kinetic tutoring. The NSLS is supported by the US Department of Energy, Division of Material Sciences and Division of Chemical Sciences. F.V.R. is a fellow of the Jane Coffin Childs Memorial Fund. J.J.S. is a Bristol-Myers Squibb Predoctoral Fellow. This work was supported in part by a grant from the US National Institutes of Health (G.J.H.) and the Louis Morin Charitable Trust (L.J.).

COMPETING INTERESTS STATEMENT

The authors declare that they have no competing financial interests.

Received 22 December 2004; accepted 9 March 2005
Published online at http://www.nature.com/nsmb/

1. Hannon, G.J. RNA interference. *Nature* **418**, 244–251 (2002).
2. Martinez, J., Patkaniowska, A., Urlaub, H., Luhrmann, R. & Tuschl, T. Single-stranded antisense siRNAs guide target RNA cleavage in RNAi. *Cell* **110**, 563–574 (2002).
3. Nykanen, A., Haley, B. & Zamore, P.D. ATP requirements and small interfering RNA structure in the RNA interference pathway. *Cell* **107**, 309–321 (2001).
4. Lee, Y.S. *et al.* Distinct roles for *Drosophila* Dicer-1 and Dicer-2 in the siRNA/miRNA silencing pathways. *Cell* **117**, 69–81 (2004).
5. Hammond, S.M., Bernstein, E., Beach, D. & Hannon, G.J. An RNA-directed nuclease mediates post-transcriptional gene silencing in *Drosophila* cells. *Nature* **404**, 293–296 (2000).
6. Meister, G. *et al.* Human Argonaute2 mediates RNA cleavage targeted by miRNAs and siRNAs. *Mol. Cell* **15**, 185–197 (2004).
7. Liu, J. *et al.* Argonaute2 is the catalytic engine of mammalian RNAi. *Science* **305**, 1437–1441 (2004).
8. Song, J.J., Smith, S.K., Hannon, G.J. & Joshua-Tor, L. Crystal structure of Argonaute and its implications for RISC slicer activity. *Science* **305**, 1434–1437 (2004).
9. Parker, J.S., Roe, S.M. & Barford, D. Crystal structure of a PIWI protein suggests mechanisms for siRNA recognition and slicer activity. *EMBO J.* **23**, 4727–4737 (2004).
10. Martinez, J. & Tuschl, T. RISC is a 5′ phosphomonoester-producing RNA endonuclease. *Genes Dev.* **18**, 975–980 (2004).
11. Schwarz, D.S., Tomari, Y. & Zamore, P.D. The RNA-induced silencing complex is a Mg^{2+}-dependent endonuclease. *Curr. Biol.* **14**, 787–791 (2004).
12. Ma, J.B., Ye, K. & Patel, D.J. Structural basis for overhang-specific small interfering RNA recognition by the PAZ domain. *Nature* **429**, 318–322 (2004).
13. Hockensmith, J.W., Kubasek, W.L., Vorachek, W.R., Evertsz, E.M. & von Hippel, P.H. Laser cross-linking of protein-nucleic acid complexes. *Methods Enzymol.* **208**, 211–236 (1991).
14. Song, J.J. *et al.* The crystal structure of the Argonaute2 PAZ domain reveals an RNA binding motif in RNAi effector complexes. *Nat. Struct. Biol.* **10**, 1026–1032 (2003).
15. Lingel, A., Simon, B., Izaurralde, E. & Sattler, M. Nucleic acid 3′-end recognition by the Argonaute2 PAZ domain. *Nat. Struct. Mol. Biol.* **11**, 576–577 (2004).
16. Tomari, Y., Matranga, C., Haley, B., Martinez, N. & Zamore, P.D. A protein sensor for siRNA asymmetry. *Science* **306**, 1377–1380 (2004).
17. Elbashir, S.M., Martinez, J., Patkaniowska, A., Lendeckel, W. & Tuschl, T. Functional anatomy of siRNAs for mediating efficient RNAi in *Drosophila melanogaster* embryo lysate. *EMBO J.* **20**, 6877–6888 (2001).
18. Elbashir, S.M., Lendeckel, W. & Tuschl, T. RNA interference is mediated by 21- and 22-nucleotide RNAs. *Genes Dev.* **15**, 188–200 (2001).
19. Stuckey, J.A. & Dixon, J.E. Crystal structure of a phospholipase D family member. *Nat. Struct. Biol.* **6**, 278–284 (1999).
20. Gray, C.H., Good, V.M., Tonks, N.K. & Barford, D. The structure of the cell cycle protein Cdc14 reveals a proline-directed protein phosphatase. *EMBO J.* **22**, 3524–3535 (2003).
21. Cox, D.N. *et al.* A novel class of evolutionarily conserved genes defined by piwi are essential for stem cell self-renewal. *Genes Dev.* **12**, 3715–3727 (1998).
22. Yang, W. & Steitz, T.A. Recombining the structures of HIV integrase, RuvC and RNase H. *Structure* **3**, 131–134 (1995).
23. Davies, J.F. 2nd, Hostomska, Z., Hostomsky, Z., Jordan, S.R. & Matthews, D.A. Crystal structure of the ribonuclease H domain of HIV-1 reverse transcriptase. *Science* **252**, 88–95 (1991).
24. Haruki, M., Tsunaka, Y., Morikawa, M., Iwai, S. & Kanaya, S. Catalysis by *Escherichia coli* ribonuclease HI is facilitated by a phosphate group of the substrate. *Biochemistry* **39**, 13939–13944 (2000).
25. Kanaya, S., Oobatake, M. & Liu, Y. Thermal stability of *Escherichia coli* ribonuclease HI and its active site mutants in the presence and absence of the Mg^{2+} ion. Proposal of a novel catalytic role for Glu48. *J. Biol. Chem.* **271**, 32729–32736 (1996).
26. Kanaya, S. & Ikehara, M. Functions and structures of ribonuclease H enzymes. *Subcell. Biochem.* **24**, 377–422 (1995).
27. Steitz, T.A. & Steitz, J.A. A general two-metal-ion mechanism for catalytic RNA. *Proc. Natl. Acad. Sci. USA* **90**, 6498–6502 (1993).
28. Beese, L.S. & Steitz, T.A. Structural basis for the 3′-5′ exonuclease activity of *Escherichia coli* DNA polymerase I: a two metal ion mechanism. *EMBO J.* **10**, 25–33 (1991).
29. Goedken, E.R. & Marqusee, S. Co-crystal of *Escherichia coli* RNase HI with Mn^{2+} ions reveals two divalent metals bound in the active site. *J. Biol. Chem.* **276**, 7266–7271 (2001).
30. Katayanagi, K., Okumura, M. & Morikawa, K. Crystal structure of *Escherichia coli* RNase HI in complex with Mg^{2+} at 2.8 Å resolution: proof for a single $Mg^{(2+)}$-binding site. *Proteins* **17**, 337–346 (1993).
31. Chapados, B.R. *et al.* Structural biochemistry of a type 2 RNase H: RNA primer recognition and removal during DNA replication. *J. Mol. Biol.* **307**, 541–556 (2001).
32. Klumpp, K. *et al.* Two-metal ion mechanism of RNA cleavage by HIV RNase H and mechanism-based design of selective HIV RNase H inhibitors. *Nucleic Acids Res.* **31**, 6852–6859 (2003).
33. Steiniger-White, M., Rayment, I. & Reznikoff, W.S. Structure/function insights into Tn5 transposition. *Curr. Opin. Struct. Biol.* **14**, 50–57 (2004).
34. Davies, D.R., Goryshin, I.Y., Reznikoff, W.S. & Rayment, I. Three-dimensional structure of the Tn5 synaptic complex transposition intermediate. *Science* **289**, 77–85 (2000).
35. Steiniger-White, M., Bhasin, A., Lovell, S., Rayment, I. & Reznikoff, W.S. Evidence for "unseen" transposase-DNA contacts. *J. Mol. Biol.* **322**, 971–982 (2002).
36. Lovell, S., Goryshin, I.Y., Reznikoff, W.R. & Rayment, I. Two-metal active site binding of a Tn5 transposase synaptic complex. *Nat. Struct. Biol.* **9**, 278–281 (2002).
37. Bujacz, G. *et al.* Binding of different divalent cations to the active site of avian sarcoma virus integrase and their effects on enzymatic activity. *J. Biol. Chem.* **272**, 18161–18168 (1997).
38. Peterson, G. & Reznikoff, W. Tn5 transposase active site mutations suggest position of donor backbone DNA in synaptic complex. *J. Biol. Chem.* **278**, 1904–1909 (2003).
39. Haley, B. & Zamore, P.D. Kinetic analysis of the RNAi enzyme complex. *Nat. Struct. Mol. Biol.* **11**, 599–606 (2004).

40. Ishizuka, A., Siomi, M.C. & Siomi, H. A *Drosophila* fragile X protein interacts with components of RNAi and ribosomal proteins. *Genes Dev.* **16**, 2497–2508 (2002).
41. Tabara, H., Yigit, E., Siomi, H. & Mello, C.C. The dsRNA binding protein RDE-4 interacts with RDE-1, DCR-1, and a DExH-box helicase to direct RNAi in *C. elegans*. *Cell* **109**, 861–871 (2002).
42. Tijsterman, M., Ketting, R.F., Okihara, K.L., Sijen, T. & Plasterk, R.H. RNA helicase MUT-14-dependent gene silencing triggered in C. elegans by short antisense RNAs. *Science* **295**, 694–697 (2002).
43. Tomari, Y. *et al.* RISC assembly defects in the *Drosophila* RNAi mutant armitage. *Cell* **116**, 831–841 (2004).
44. Motamedi, M.R. *et al.* Two RNAi complexes, RITS and RDRC, physically interact and localize to noncoding centromeric RNAs. *Cell* **119**, 789–802 (2004).
45. Meister, G. & Tuschl, T. Mechanisms of gene silencing by double-stranded RNA. *Nature* **431**, 343–349 (2004).
46. Haley, B., Tang, G. & Zamore, P.D. In vitro analysis of RNA interference in *Drosophila melanogaster*. *Methods* **30**, 330–336 (2003).
47. Otwinowski, Z. & Minor, W. Processing of X-ray diffraction data collected in oscillation mode. *Methods Enzymol.* **276**, 307–326 (1997).
48. Jones, T.A. & Kjeldgaard, M. Electron-density map interpretation. *Methods Enzymol.* **277**, 173–208 (1997).
49. Brünger, A.T. *et al.* Crystallography & NMR system: a new software suite for macromolecular structure determination. *Acta Crystallogr. D* **54**, 905–921 (1998).
50. Ryter, J.M. & Schultz, S.C. Molecular basis of double-stranded RNA-protein interactions: structure of a dsRNA-binding domain complexed with dsRNA. *EMBO J* **17**, 7505–7513 (1998).
51. Esnouf, R.M. An extensively modified version of MolScript that includes greatly enhanced coloring capabilities. *J. Mol. Graph.* **15**, 132–134 (1997).
52. Bacon, D.J. & Anderson, W.F. A fast algorithm for rendering space-filling molecule pictures. *J. Mol. Graph.* **6**, 219–220 (1988).
53. Merritt, E.A. & Murphy, M.E.P. Raster3D version 2.0—a program for photorealistic molecular graphics. *Acta Crystallogr. D* **50**, 869–873 (1994).